

## EVAPORATION RATES AND SURFACE PROFILES ON HETEROGENEOUS SURFACES WITH MASS TRANSFER AND SURFACE REACTION†

M FLYTZANI-STEPHANOPOULOS and L D SCHMIDT

Department of Chemical Engineering and Materials Science, University of Minnesota, Minneapolis, MN 55455, U S A

(Received 26 April 1978, accepted 9 June 1978)

**Abstract**—Models incorporating surface reaction and diffusion of volatile products through a boundary layer are developed to calculate effective rates of evaporation and local surface profiles on surfaces having active and inactive regions. The coupling between surface heterogeneities with respect to a particular reaction and external mass transfer may provide a mechanism of the surface rearrangement and metal loss of catalysts encountered in several systems of practical interest. Calculated transport rates for the volatilization of Pt in oxidizing environments and the rearrangement of this metal during the ammonia oxidation reaction are found to agree well with experimental data.

### INTRODUCTION

The alteration of the topography of a solid surface at elevated temperatures in inert or mildly active atmospheres (thermal etching) as well as the influence of solid-gas reactions upon surface rearrangements (catalytic etching) are well known phenomena that have been studied since the turn of the century [1, 2]. In particular, the interest in the latter stems from its close association with catalyst activity, catalyst metal loss, and the sintering process in supported catalysts.

Thermal etching has been analyzed almost exclusively from minimum surface free energy considerations [3]. Mullins [4, 5] has presented a theory which accounts for the development of several surface morphologies such as grain-boundary grooves and growth of linear facets on heated polycrystals, on the assumption that they are energetically induced. Under idealized conditions, standard forms of localized surface profiles were obtained for the cases where surface diffusion or evaporation-condensation was the operative mechanism.

However, experimental studies of thermal etching under suppressed evaporation conditions, first performed by Hondros and Moore [6], have led to disagreement as to whether equilibrium faceting alone controls the etching process for "open" systems in which a steady loss of material from the surface of the sample may take place. Moreover, for environments where chemical reactions are possible, the expressions which describe mass transport can be altered by the superposition of a chemical interaction onto a mechanism strictly driven by capillarity.

The development of surface roughness and concomitant catalyst erosion are important factors in many industrial processes, in which steady losses of costly catalyst material accompany the reaction. Another situation in which mass transport occurs in chemically reac-

tive environments is the movement of solids through the gas phase by means of heterogeneous reversible reactions [7]. In the case of metal loss a well known example in oxidizing atmospheres is that of the platinum metals which form volatile oxides. Also, solid oxides such as BeO, WO<sub>3</sub>, and others can react with water vapor to produce volatile hydroxides.

In these and other similar processes the most important factor is the transport of surface material, and for this reason several experimental and theoretical studies have appeared in the literature on measurements of evaporation rates and analysis of kinetics, for example, the oxidation kinetics of Pt, W, Cr<sub>2</sub>O<sub>3</sub>, etc. Bartlett [8] developed an expression for evaporation rates in cases where convective diffusion and surface reaction are coupled by considering equilibrium data for the reaction and dimensionless fluid correlations.

In all such studies, a uniformly active surface has been assumed, and changes in topography which occur in many of these processes, probably through gaseous mass transfer from some regions of the surface to others, are ignored. It is well known, however, that most surfaces exhibit heterogeneity with respect to their interactions with adsorbing gases. In a recent paper by Löffler and Schmidt [9] the coupling between mass transfer and surface heterogeneities was considered and effective catalytic reaction rates and selectivities were calculated.

We consider in this paper simple models incorporating both surface heterogeneities and external mass transfer to see how they may affect evaporation rates and surface rearrangements under conditions where the operative mechanism is boundary-layer diffusion of a volatile product species.

### MODELS

A simple two-dimensional geometry will be assumed in all cases for a solid surface containing regions of different reactivities. Consider a system consisting of active stripes of width  $2l$  and length much greater than

†This work partially supported by NSF under Grant No ENG75-01918

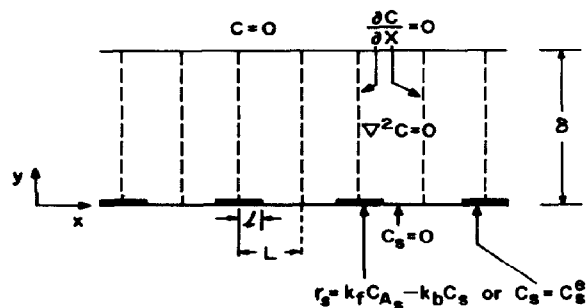


Fig. 1 Sketch of system and parameters used for calculations of evaporation rates and surface profiles

$2l$ , which are evenly distributed on an otherwise inert surface (Fig. 1), covered by a stagnant film of some gas reactive with the surface of thickness  $\delta$ . An actual surface may consist of active regions of various shapes which are randomly distributed and/or widely separated, and flow conditions may be such that the above defined system becomes oversimplified. However, it should correspond qualitatively to several realistic situations in which mass transfer effects are not strongly sensitive to the exact shapes of active regions, surface roughness is small compared to boundary layer thickness, etc.

We assume that a vapor species (such as a volatile metal oxide) involving the surface constituent is formed exclusively on the active stripes and diffuses through the film with diffusivity  $\mathcal{D}$  to inactive regions and also through the boundary layer where it is carried away by the gas flow stream. The concentration of the gaseous product on the inactive stripes will be zero since it is assumed that all molecules of this species that strike the hot surface are unstable and dissociate instantly so that solid material is being deposited on the inactive regions during this process. We are interested in overall vaporization rates and rates of material deposition per unit surface area for specified kinetics on individual patches. To evaluate these quantities, we need concentrations and their derivatives (fluxes) as a function of position in the boundary.

A steady state mass balance on the gaseous product of concentration  $C$  in the domain shown in Fig. 1 with  $y=0$  along the surface, and  $x=0$  at the center of an active stripe gives

$$\nabla^2 C = \frac{\partial^2 C}{\partial x^2} + \frac{\partial^2 C}{\partial y^2} = 0 \quad (1)$$

with boundary conditions

$$\frac{\partial C}{\partial x} = 0, \quad x = 0 \text{ and } x = L, \quad \text{all } y \quad (2a)$$

$$\frac{\partial C}{\partial y} = -\frac{r}{\mathcal{D}}, \quad y = 0 \text{ and } 0 < x < l \quad (2b)$$

$$C = 0, \quad y = 0 \text{ and } l < x < L \quad (2c)$$

and

$$C = 0, \quad y = \delta, \quad \text{all } x \quad (2d)$$

Conditions (2a) are imposed by symmetry. The boundary condition (2c) gives a zero concentration of the volatile product on the inactive stripes (although there is lateral diffusion) because of the assumed rapid dissociation of this compound on the hot surface back to its solid and gas constituents.

We shall first consider the simple case of a completely diffusion limited reaction on a surface with stripes, then examine the case of a finite reaction rate and illustrate calculations of concentration profiles. Next, we shall present mass transport rates and plot the surface profiles predicted in each case. Finally, numerical examples will be given to show the applications of the model and compare with existing experimental data.

### Mass transfer control

In this section we consider the situation where mass transfer from the active surface region is the limiting step. A reversible reaction occurs on the active stripes over which a fast equilibrium is attained so that the boundary condition of eqn (2b) for the concentration  $C$  of the produced gaseous compound becomes  $C(y=0, 0 < x < l) = C_s^e$ . We introduce the following dimensionless variables to solve the diffusion problem

$$\xi = x/\delta, \quad \eta = y/\delta, \quad u = C/C_s^e \text{ and } u_s = C_s/C_s^e$$

where subscript  $s$  refers to values on the solid surface and superscript  $e$  to equilibrium values at a given temperature and pressure.

The analytical solution to this boundary-value problem can be found by separation of variables. In a series form this solution is

$$u(\xi, \eta) = (1 - \eta) \frac{l}{L} + \sum_{k=1}^{\infty} \frac{2}{k\pi} \frac{\sin(k\pi l/L)}{\sinh(k\pi \delta/L)} \sinh\left(k\pi \frac{\delta}{L} (1 - \eta)\right) \cos\left(k\pi \frac{\delta}{L} \xi\right) \quad (3)$$

The series in eqn (3) does not converge uniformly, and its term by term differentiation at  $\eta=0$  is not allowed [10]. However, one can still evaluate derivatives of the form  $(\partial u / \partial \eta)_{\eta=0}$  which are needed to calculate transport rates (see eqns 9 and 11) either numerically by taking a very fine grid of points close to the discontinuity or analytically by approximating the step function at  $\eta=0$  by a continuous function with a small ramp.

Two independent dimensionless parameters appear in this model: the fraction of active surface  $l/L$  and the ratio of the boundary layer thickness to half the distance between stripes,  $\delta/L$ . We have calculated concentrations at the various points of the domain for several combinations of these parameters. A total of one-hundred terms of the series in eqn (3) was considered in all cases.

For typical values of the parameter  $l/L$ , we can examine the effect of changing  $\delta/L$  on the concentration of the produced species over the active and inactive regions throughout the boundary layer. An example is

### MASS TRANSFER CONTROL

$l/L=0.5$

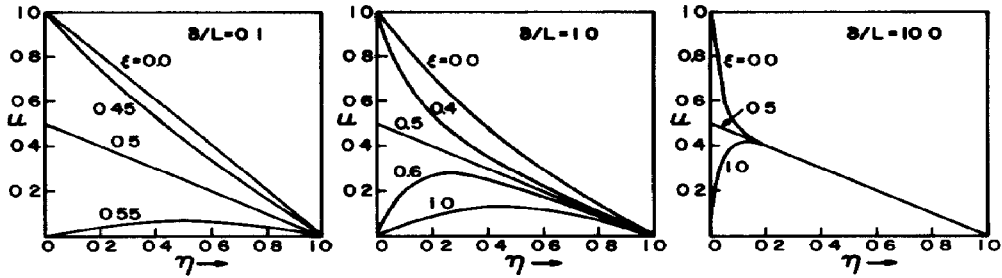


Fig 2 Effect of  $\delta/L$  on the dimensionless concentration  $u$  of the product species vs  $\eta$  for  $l/L = 0.5$  and fixed values of  $\xi$  in the diffusion limited case (eqn 3)

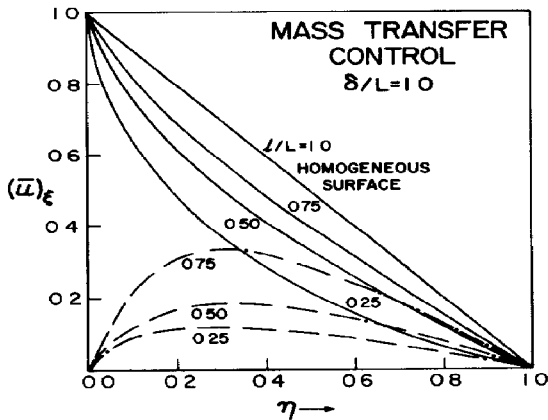


Fig 3 Effect of  $l/L$  on the product concentration averaged over all values of  $\xi$  vs  $\eta$  for  $\delta/L = 1.0$  in the diffusion limited case (eqn 3)

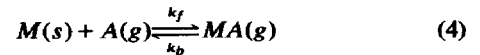
shown in Fig 2 where concentrations are plotted vs  $\eta$  for fixed values of  $\xi$ , for  $\delta/L = 0.1, 1.0, \text{ and } 10.0$ , and  $l/L = 0.5$

Figure 3 illustrates effects of varying  $l/L$  for a particular  $\delta/L$ . Here, average concentrations with respect to  $\xi$  were calculated and plotted vs  $\eta$  for several  $l/L$  and  $\delta/L = 1.0$ . In a following section we shall examine the effect that a heterogeneous surface has upon evaporation rates as compared with a uniformly active surface with  $l/L = 1.0$

In Fig 4(a) contours of equal concentrations are drawn through the points of the  $\xi - \eta$  domain, for  $l/L = 0.5$  and  $\delta/L = 1.0$

#### Finite reaction rates

We consider next the situation where a heterogeneous reversible reaction occurs on the active stripes of the solid surface,



with a slow reaction rate given by the expression

$$r_{\text{surface}} = k_f C_A - k_b C_s = -\mathcal{D} \left( \frac{\partial C}{\partial y} \right)_{y=0} \quad (5)$$

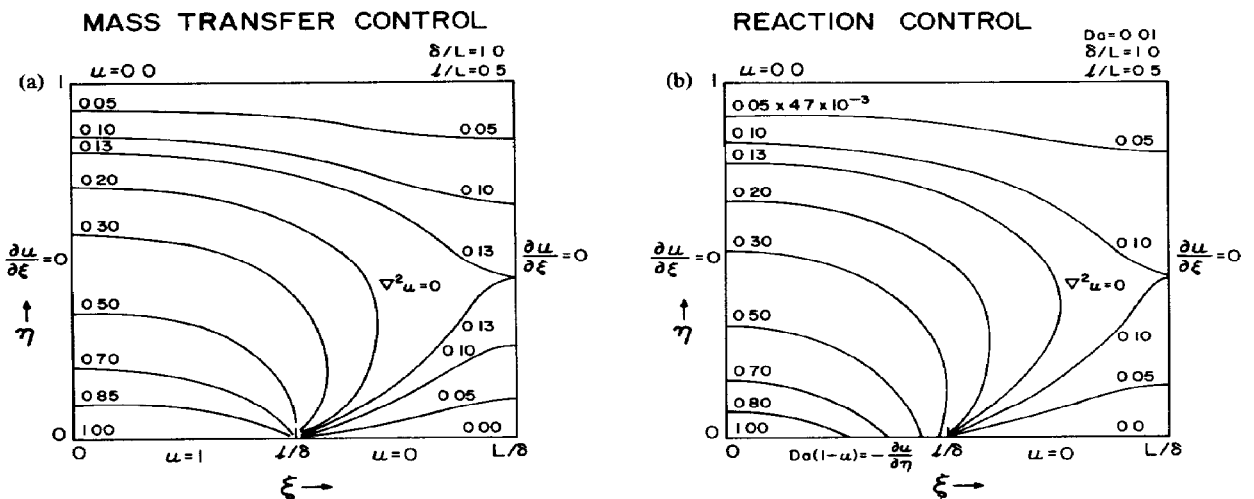


Fig 4 (a), Contours of product concentrations in the  $\xi - \eta$  domain for  $\delta/L = 1.0$  and  $l/L = 0.5$  in the diffusion limited case, (b), Same as in (a) but for reaction control with  $D_a = 0.01$ . Note the factor  $4.7 \times 10^{-3}$  multiplying all dimensionless concentrations and the different behavior close to the discontinuity at  $\xi = l/\delta$

$C_A$  in eqn (5) denotes the concentration of the reactant gaseous species  $A$  which is approximately uniform throughout the domain if the rate is slow and  $C_A \gg C_s$ . The specific rate constants  $k_f$  and  $k_b$  involving the forward and back rates of the reaction are related through the equilibrium constant,  $K_{eq}$  for the reaction of eqn (4)

$$K_{eq} = \frac{k_f}{k_b} \quad (6)$$

It is assumed that the product MA molecules are dissociated on striking the catalyst surface, and consequently  $k_b$  is the surface collision frequency of MA molecules based on gas kinetics

By introducing in eqn (5) the same dimensionless variables as in the previous section, and since  $K_{eq} = (C_s^e/C_A)$ , we obtain

$$D_a(1 - u_s) = - \left( \frac{\partial u}{\partial \eta} \right)_{\eta=0} \quad (7)$$

where  $D_a = (k_b \delta / \mathcal{D})$ , is a Damkohler number that expresses the ratio of the backward reaction rate constant to mass transfer coefficients

Equation (7) is used as the boundary condition on the active region, and the boundary-value problem is solved numerically by a finite-difference approximation using either  $20 \times 20$  or  $40 \times 40$  matrices. In this case there are three dimensionless variables,  $l/L$ ,  $\delta/L$ , and the Damkohler number,  $D_a$  defined above. For  $D_a > 20$ , the diffusion controlled situation is approached and in the limit, for very large  $D_a$ , the analytical solution discussed in the previous section is appropriate. Thus, we have compared values of the concentrations from both calculations at the same  $\delta/L$  and  $l/L$  and using a  $D_a = 10000$  for the numerical solution to find an accuracy better than  $\sim 95\%$ . Concentrations and rates are believed to be accurate within a few per cent in all calculations involving other values of the parameters.

Figure 4(b) illustrates contours of equal concentrations in the  $\xi - \eta$  domain, in a reaction limited case, with  $D_a = 0.01$ ,  $\delta/L = 1.0$ , and  $l/L = 0.5$ . The effect of  $D_a$  on the actual values of concentrations can be observed by comparing this plot with Fig 4(a), which gives the concentration profiles at the same  $\delta/L$  and  $l/L$  but in the diffusion controlled situation.

It is instructive at this point to consider the case of a uniformly active surface. Equation (7) is then the appropriate boundary condition for the whole surface ( $\eta = 0$ , all  $\xi$ ), and the diffusion problem can be solved analytically to obtain

$$u = \frac{D_a}{1 + D_a} (1 - \eta), \quad (8)$$

which shows that the concentration of the produced species falls linearly through the boundary layer with a slope approaching unity in the mass transfer limited region (for large  $D_a$ 's)

#### MASS TRANSFER RATES

From concentration profiles obtained numerically or analytically by solving eqns (1) and (2) in the reaction

and diffusion limited cases respectively, we can calculate effective mass transport rates per unit surface area on stripes of half-width  $L$ .

At steady-state, the total production rate (by surface reaction) must be equal to the evaporation rate through the top of the boundary layer and the rate of deposition of solid material on the inactive region (by dissociation of the product species).

The effective total rate per unit width  $L$  of production of solid from the active surface is calculated from the equation

$$\bar{r}_i = - \frac{\mathcal{D}}{L} \int_0^l \left( \frac{\partial C}{\partial y} \right)_{y=0} dx = - \frac{\mathcal{D} C_s^e}{L} \int_0^{l/\delta} \left( \frac{\partial u}{\partial \eta} \right)_{\eta=0} d\xi \quad (9)$$

Similarly, the evaporation and deposition rates are given by

$$\bar{r}_e = - \frac{\mathcal{D} C_s^e}{L} \int_0^{l/\delta} \left( \frac{\partial u}{\partial \eta} \right)_{\eta=1} d\xi \quad (10)$$

and

$$\bar{r}_d = \frac{\mathcal{D} C_s^e}{L} \int_{l/\delta}^{L/\delta} \left( \frac{\partial u}{\partial \eta} \right)_{\eta=0} d\xi \quad (11)$$

We can express the ratio of the evaporation rate of the product to the total rate of production from the heterogeneous surface by  $\alpha_e = \bar{r}_e / \bar{r}_i$ , and observe how this changes with the different parameters. For a uniformly active surface we obviously have  $\bar{r}_e = \bar{r}_i$  and  $\alpha_e = 1$ .

In the latter case an analytical expression for the evaporation rate is found from eqns (8) and (10),

$$\bar{r}_e = \bar{r}_i = \frac{D_a}{1 + D_a} \left( \frac{\mathcal{D} C_s^e}{\delta} \right) \quad (12)$$

It is seen, therefore, that for a uniformly active surface the theoretical eqn (12) can be applied directly to calculate vaporization rates in any pressure region, and under various flow conditions, this equation requires only equilibrium thermodynamic data and the boundary layer thickness which can be obtained from semi-empirical correlations.

In the diffusion limited case which has an analytical solution, eqns (3) and (10) give evaporation rates,  $\bar{r}_e = l/L (\mathcal{D} C_s^e / \delta)$ , lower than for a uniformly active surface (eqn (12) with  $D_a \rightarrow \infty$ ) by exactly the fraction of active surface,  $l/L$ . Thus, in this regime an upper bound to the rate of metal loss is predicted by considering the surface as homogeneous.

Effective transport rates for heterogeneous surfaces are plotted in Fig 5 vs  $\delta/L$ , for  $l/L = 0.5$ , in the diffusion control case. For comparison, rates from a homogeneous surface are also shown in the same figure.

Figure 6 illustrates the variation of evaporation rates with Damkohler number. The solid curves are drawn through calculated values of  $\bar{r}_e$ , for  $l/L = 0.5$ , and dashed curves are for rates at  $l/L = 1.0$  (homogeneous surface). In the region of small  $D_a$ 's (reaction control) rates increase approximately linearly with increasing Damkoh-

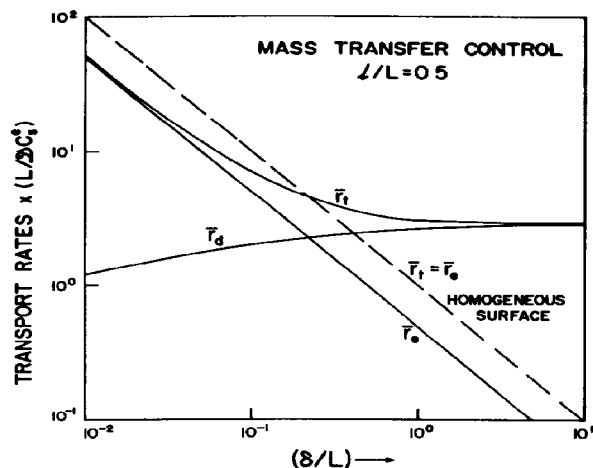


Fig 5 Effective transport rates (eqns 9-12) plotted vs  $\delta/L$  for  $l/L = 0.5$  under mass transfer control ( $D_a \rightarrow \infty$ )

ler number, while in the diffusion control regime, there is only a small increase in the evaporation rates with  $D_a$ . The rates plotted in Fig 6 are for three values of the parameter  $\delta/L$ . We see that as  $\delta/L$  increases, the difference between evaporation rates from a homogeneous surface and those from a surface with  $l/L = 0.5$  becomes more and more pronounced especially in the reaction control region (because for large  $\delta/L$ , there is a relatively higher deposition rate on the inactive stripes)

### SURFACE PROFILES

This model allows an estimation of surface profiles through the assumption of surface heterogeneity because, while there is a constant removal rate on the active regions of the surface (active stripes in the present model), there is also a concomitant built-up rate on the inactive region at steady-state conditions. The shapes of the surface profiles will depend on the parameters involved in the model.

Using our analytical and numerical calculations, we found the slopes of concentrations of the produced species at all points of the surface ( $\eta = 0$ ). These are of course negative on the active region and positive on the inactive stripes. Figure 7(a) shows plots of the derivative  $(\partial u / \partial \eta)_{\eta=0}$  vs  $\xi$  in the mass transfer controlled situation for  $l/L = 0.5$  and for three values of the parameter  $\delta/L = 0.1, 1.0$  and  $10.0$ . For small values of  $\delta/L$ , it is observed that a strong variation occurs near the point of discontinuity and there is also a large deposition of material close to this point on the inactive part of the surface ("lip" or "hillock" formation). As  $\delta/L$  increases, however, the profile becomes more and more uniform because material evaporates almost equally from all points of the active stripe and is deposited uniformly again on the inactive region. Note that in this case curves are almost symmetrical since the evaporation rates for large  $\delta/L$  are very low.

Surface profiles were also calculated for other conditions, and for various Damkoehler numbers. In the reaction limited regime, with  $D_a = 0.01$ , the results are shown in Fig 7(b). Here we have again chosen  $l/L = 0.5$  and

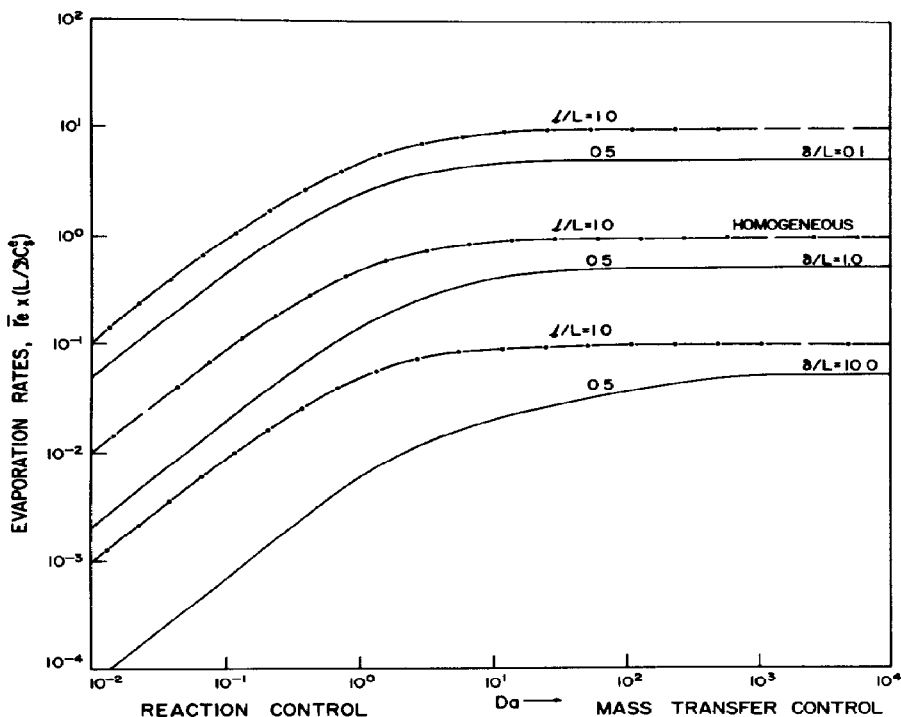


Fig 6 Evaporation rates vs Damkoehler number,  $D_a$  for  $\delta/L = 0.1, 1.0$ , and  $10.0$ . Solid curves are for heterogeneous surfaces with  $l/L = 0.5$ , while dashed curves are for  $l/L = 1.0$  (homogeneous surfaces)

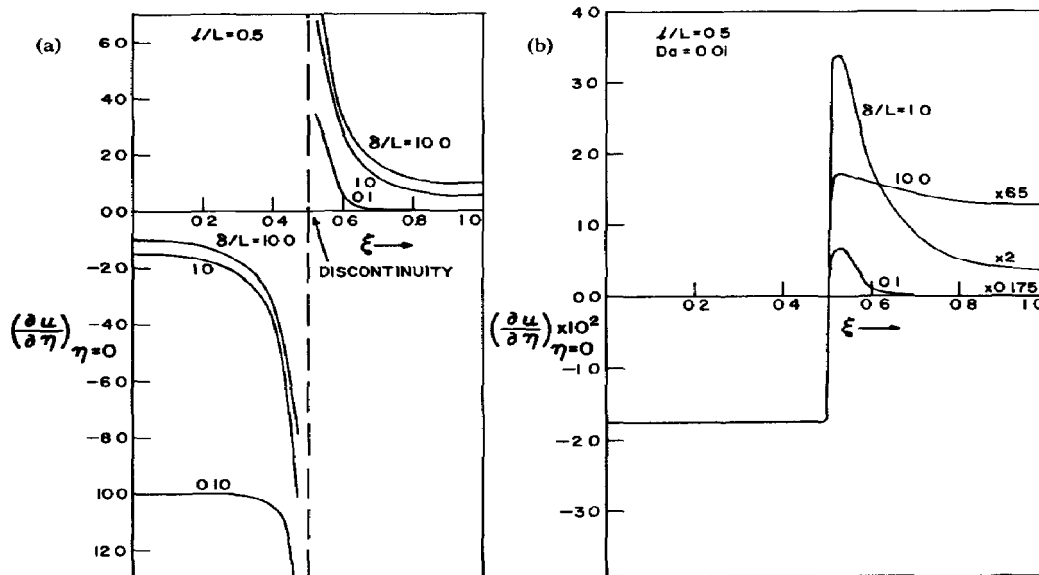


Fig 7 (a), Surfaces profiles in the diffusion limited case for  $l/L = 0.5$  and  $\delta/L = 0.1, 1.0$  and  $10.0$  (b), Surface profiles for the reaction control case with  $D_a = 0.01$  and same  $l/L$  and  $\delta/L$  parameters as in (a), reduced to the same recession profile on the active region by the shown scaling factors

plotted values of the slopes  $(\frac{\partial u}{\partial \eta})_{\eta=0}$  on the surface vs  $\xi$ , for the same  $\delta/L$  values as in Fig 7(a). In this case we have averaged the profiles and reduced them to the same value of  $(\frac{\partial u}{\partial \eta})_{\eta=0}$  in order to get a better picture of the profiles on the inactive region. On each curve the numbers by which actual deposition and recession profiles were multiplied are given. Comparing these relative profiles, we see that for the same recessed active surface, the built-up material on the inactive appears like a sharp hillock close to the point of discontinuity, for  $\delta/L = 0.1$ , while for  $\delta/L = 1.0$ , relatively more material is deposited toward the end of the inactive stripe, and for  $\delta/L = 10.0$  the built-up is almost uniform with  $\xi$ .

These profiles, while actually observed in situations where erosion of the solid is known to occur, by no means describe all morphologies observed in thermal and catalytic etching. We may use them, however, as a first approximation in cases of practical interest, some of which are discussed in the following section, to see whether average heights of deposited material are of the order of experimental values after specified periods of time.

#### APPLICATIONS

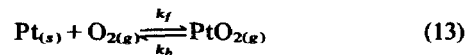
The models developed in the previous sections may be applied to systems in which a solid substance (uniformly or nonuniformly active) reacts with a gas to form volatile products which then undergo the reverse reaction, reforming the solid at a different location in the system. Chemical transport reactions of this kind include formation and decomposition of oxides (e.g. platinum metals oxidation), metal and oxide transport in water vapor (e.g. W, BeO, WO<sub>3</sub>, SiO<sub>2</sub>), oxide transport in the presence of oxygen (e.g. IrO<sub>2</sub>, RuO<sub>2</sub>, Cr<sub>2</sub>O<sub>3</sub>) and others [7].

In these processes it is assumed that the solid does not

possess an appreciable vapor pressure at the applied temperatures, so that it is transported as a compound rather than by sublimation.

#### Platinum oxidation

Platinum oxidizes at measurable rates for temperatures above  $\sim 800$  C to produce a volatile species, PtO<sub>2</sub> [11]



At steady state, the oxidation rate for the surface reaction given by eqn (13) is,

$$r_s = k_f C_{\text{O}_2,s} - k_b C_{\text{PtO}_2,s} \quad (14)$$

where  $r_s$  is in [g/cm<sup>2</sup> sec],  $k_f$  and  $k_b$  are the forward and back specific rate constants in [cm/sec],  $C_{\text{PtO}_2,s}$  is the oxide concentration on the metal surface in [g/cm<sup>3</sup>], and  $C_{\text{O}_2,s} = P_{\text{O}_2,s} M_{\text{O}_2} / RT_g$ , the oxygen concentration in [g/cm<sup>3</sup>], assumed unperturbed as the surface is approached, i.e.  $C_{\text{O}_2,s} = C_{\text{O}_2,g}$ . Values for the equilibrium constant of this reaction  $K_{eq}$  can be taken from the work of Alcock and Hooper [11]. For a condensation coefficient of unity for the dissociation of the unstable PtO<sub>2</sub> molecules upon striking the hot platinum surface, we can calculate  $k_b$ , in eqn (14) by the expression,

$$k_b = (2\pi MRT)^{-1/2} RT_g \quad (15)$$

where  $M$  is the molecular weight of PtO<sub>2</sub>.

Assuming a heterogeneous surface, we can now apply our diffusion model to the oxidation of platinum and calculate evaporation and deposition rates from eqns (10)

and 11) The diffusion coefficients are estimated from the Chapman-Enskog equation[12] The boundary layer thickness  $\delta$ , can be calculated from an expression of the form,  $\delta = w/\text{Nu}_m$  [13], where  $w$  is a characteristic dimension of the sample, and  $\text{Nu}_m$ , the Nusselt number for mass transfer, can be obtained from published free or forced convection correlation curves[14, 15]

**Evaporation rates** Several years ago Fryburg and Petrus[16] employed electrically heated platinum ribbons in oxygen or air to study experimentally the kinetics of the oxidation of platinum

Bartlett[8] in 1967, considered the coupling of convective diffusion and surface reaction on a uniformly active platinum surface, and calculated platinum evaporation rate isotherms In static oxygen at 1060°C his calculated oxidation rates agreed well with Fryburg's experimental data over the entire pressure range for ribbons 0.0287 cm wide

In this case, the assumption of a uniformly active ( $l/L = 1$ ) platinum surface may be quite good However, Fryburg reported that evaporation rates were lower from crystals with {111} orientation from the polycrystalline ribbons Also microscopic examination of the ribbons after reaction revealed some striated grains and others that were smooth but dotted with small pits Thus, it seems worthwhile to apply our models of a heterogeneous surface to calculate rates of platinum evaporation and redeposition

Assuming that the active region comprises most of the surface except for some spots where normal oxidation is inhibited, we have calculated  $\bar{r}_e$  and  $\bar{r}_d$  for a Pt ribbon 0.0287 cm wide 1 atm of oxygen and 1060°C The values of the parameters  $l/L$  and  $\delta/L$  were taken equal to 0.9 and 15 respectively (for  $\delta \sim 300 \mu$  and  $L = 20 \mu$ ) Since  $D_a > 150$  at these conditions, the model for mass transfer control was applied The evaporation rate,  $\bar{r}_e$ , is thus equal to  $8.8 \times 10^{-6}$  cm Pt/hr in good agreement with the experimental value ( $\sim 1.2 \times 10^{-5}$  cm Pt/hr) The rate of deposition,  $\bar{r}_d$ , was found equal to  $3 \times 10^{-4}$  cm/hr, that is, in about one hour the height of the hillocks will be of the order of 2–3  $\mu$ , again within the range of experimental observations

### NH<sub>3</sub> oxidation on platinum

**Faceting** In a recent publication[17] we described the morphological changes induced on single crystal spheres of platinum metals used to catalyze the NH<sub>3</sub> oxidation reaction at a total pressure of 1 atm Under autothermal conditions, facets of 1–3  $\mu$  size were observed on the platinum spheres We suggested that a possible mechanism of faceting may be the boundary layer transport of PtO<sub>2</sub> formed selectively on regions that are the least active with respect to the main reaction (NH<sub>3</sub> oxidation)

We can apply the models developed here to calculate rates of platinum deposition and explain faceting in terms of this mechanism As an example, let us consider a 10% NH<sub>3</sub> in air mixture ( $P_{O_2} = 0.18$  atm) for a catalyst temperature of 900°C For a sphere of 200  $\mu$  diameter and low flow velocities we estimate  $\delta \sim 100 \mu$  Then  $D_a \sim 60$ , and for  $l/L = 0.5$ , the rate of deposition,  $\bar{r}_d$  can be found from Fig 5 Thus,  $\bar{r}_d = 2.8(\mathcal{D}C_s^e/lL)(3600/\rho_{Pt}) =$

$10^{-4}$  cm Pt/hr, where  $\mathcal{D} \sim 0.8$  cm<sup>2</sup>/sec,  $C_s^e = 5.33 \times 10^{-11}$  g Pt/cm<sup>3</sup>,  $\rho_{Pt} = 21.4$  g/cm<sup>3</sup>, and  $L$  was taken equal to 2  $\mu$  This value for  $\bar{r}_d$  is of exactly the same order of magnitude with observed rates of faceting[17]

**Putting** When the platinum spheres were heated well above the adiabatic temperature for conditions otherwise the same as discussed previously, randomly distributed pits appear on the surface after only a short time of reaction[17] We can calculate  $\bar{r}_d$ , in this case, for  $T = 1400^\circ\text{C}$ ,  $l = 2 \mu$ , and  $l/L = 0.1$  (i.e. by assuming that oxidation of platinum is enhanced at some spots probably because of higher local temperatures) For  $\delta/L = 5$ ,  $l/L = 0.1$ , and  $D_a \sim 45$ , we used the model for mass transfer control to find  $\bar{r}_d \sim 10^{-3}$  cm Pt/hr Thus, it would take 15–20 min for pits of  $\sim 3 \mu$  to form, as we have observed experimentally

**Metal loss** Rates of platinum loss at several temperatures during ammonia oxidation were calculated by Nowak[18] with the assumption that the metal loss was due to reaction (13) followed by transport of gaseous PtO<sub>2</sub> away from the surface Following the method used by Bartlett[8], he calculated oxidation rates for infinite platinum cylinders in forced convective flow under the conditions used by Handforth and Tilley[19] in their measurements of platinum loss during ammonia oxidation These rates were found to be greater than the observed rates by a factor of about four in the temperature range of 500–1400°C where mass transport was the rate limiting step[18]

Our model of a heterogeneous surface would predict lower evaporation rates (by the factor  $l/L$ ) than those from a uniformly active surface ( $l/L = 1$ ) assumed by Nowak, thus bringing the rates closer to the experimental values Moreover, it would allow an estimation of the rates of surface roughening which is considerable and occurs simultaneously with metal loss in the industrial ammonia oxidation converters

We also note that these models predict lower rates for larger crystals in agreement with experiments[17] Also, the effect of higher flow velocities would be higher rates of evaporation in the mass transfer control regime

**Acknowledgements**—We would like to thank Messrs G. N. Stephanopoulos and R. Gorte for very helpful discussions

### REFERENCES

- [1] Moore A. J. W., In *Metal Surfaces* (Edited by D. Roberston and N. A. Gjostein), p. 155. Am. Soc. for Metals, Metals Park, Ohio 1963
- [2] Cunningham R. E. and Gwathmey A. T., *Adv. Cat.* 1958 **10**, 57
- [3] Herring C., In *Structure and Properties of Solid Surfaces* (Edited by R. Gomer and C. S. Smith), p. 5. Chicago, University of Chicago Press 1953
- [4] Mullins W. W., *J. Appl. Phys.* 1957 **28**, 333
- [5] Mullins W. W., *Phil. Mag.* 1961 **6**, Ser. 8, 1313
- [6] Hondros E. D. and Moore A. J. W., *Acta Met.* 1960 **8**, 647
- [7] Schäfer H., *Chemical Transport Reactions* (trans. by H. Frankfort), Chap. 3. Academic Press, New York 1964
- [8] Bartlett R. W., *J. Electrochem. Soc.* 1967 **114**(6), 547
- [9] Löffler D. G. and Schmidt L. D., *A.I.Ch.E.J.* 1975 **21**, 786
- [10] Weinberger H. F., *A First Course in Partial Differential Equations*, Chap. IV. Xerox College, Lexington, Massachusetts 1965

- [11] Alcock C B and Hooper G W, *Proc Roy Soc* 1960 **A254** 551
- [12] Hirschfelder J O, Curtiss C F and Bird R B, *Molecular Theory of Gases and Liquids*, p 539 Wiley, New York 1954
- [13] Skelland A H P, *Diffusional Mass Transfer*, Chap 5 Wiley, New York 1974
- [14] Jakob M, *Heat Transfer*, 9th Edn, Vol 1, p 525 Wiley, New York 1964
- [15] Bird R B, Stuart W E and Lightfoot E N, *Transport Phenomena*, p 408 Wiley, New York 1960
- [16] Fryburg G C and Petrus H M, *J Electrochem Soc* 1961 **108** 496
- [17] Flytzani-Stephanopoulos M, Wong S and Schmidt L F, *J Cat* 1977 **49** 51
- [18] Nowak E J, *Chem Engng Sci* 1966 **21** 19, 1969 **24** 421
- [19] Handforth S L and Tilley J N, *Ind Engng Chem* 1934 **26** 1287